# Soliton-Mediated Electron Transfer and Electric Transport Arising from Coupling Electron Quantum Mechanics to Nonlinear Elasticity in Anharmonic Crystal Lattices

**M.G. Velarde, W. Ebeling, and A.P. Chetverikov**

**Abstract** After recalling features of solitons in the Toda (more precisely an adapted Morse-Toda) lattice a succint discussion is provided about the stability of such solitons when the lattice is heated up to physiological temperatures for values of parameters typical of bio-macro-molecules. Then the discussion is focused on the soliton trapping of an added *excess* (originally free) electron thus creating the solectron electric carrier. Results are presented for 1d- and 2d-anharmonic crystal lattices.

**Keywords** Cristal Lattices • Solitons • Electric transport • Heating

## 1 Background: Solitons

The study of anharmonic lattices owes much to the seminal work done by Fermi, Pasta and Ulam (1955). They tried numerically albeit with no success to explain equipartition of energy (of paramount importance in statistical mechanics) by using the first few non-Hookean corrections to linear elasticity as a mechanism to allow energy sharing and exchange between harmonic modes otherwise non-interacting. The difficulty was clarified by Zabusky and Kruskal (1965) and Zabusky (2005) who studied solitary waves, their overtaking collisions in such anharmonic lattices

M.G. Velarde (✉)
Instituto Pluridisciplinar, Paseo Juan XXIII, 1, Madrid-28040, Spain
e-mail: mgvelarde@pluri.ucm.es

W. Ebeling
Institut für Physik, Humboldt-Universität Berlin, Newtonstrasse, 15, Berlin-12489, Germany
e-mail: ebeling@physik.hu-berlin.de

A.P. Chetverikov
Department of Physics, Saratov State University, Astrakhanskaya, 83, Saratov-410012, Russia
e-mail: ChetverikovAP@info.sgu.ru

M. Wiercigroch and G. Rega (eds.), *IUTAM Symposium on Nonlinear Dynamics for Advanced Technologies and Engineering Design*, IUTAM Bookseries (closed) 32, DOI 10.1007/978-94-007-5742-4_4,
© Springer Science+Business Media Dordrecht 2013

and their continuum counterpart. In view of their remarkable particle-like behavior, these waves reappearing unaltered following collisions, the hallmark of their dynamics, they denoted them by solitons (solit/solitary wave; on/like in electron, proton, etc.). In fact, before the discovery of the soliton, Visscher and collaborators numerical computations (Payton et al. 1967) had revealed "soliton-like" mediated behavior and enhanced heat transport. Solitary waves and solitons, found also in other realms of science, appear as potential "universal" carriers of almost anything (del Rio et al. 2007; Nayanov 1986) (like surf waves/non-topological solitons in the ocean or bores/topological solitons in rivers). Of particular interest to us here is the model-lattice invented by Toda (1989) for which analytical, exact solutions are known.

Let us recall how solitons appear in the anharmonic Toda lattice. Consider an one-dimensional (1d) lattice of units (equal masses, $m$ and $m = 1$ for simplicity) interacting with their nearest-neighbors via a potential $U(x)$. Then, classically, for the displacement of the $n$th-lattice unit/particle from its equilibrium position, Newton's equations are

$$\ddot{x}_n = U'(x_{n+1} - x_n) - U'(x_n - x_{n-1}), \tag{1}$$

where $x_n$ denotes displacement (depending on circumstances it is of interest to focus on local lattice deformations or on gradient of displacements) of the unit at site "$n$". A dash indicates a derivative with respect to the argument. No on-site dynamics or structure is considered. There are cases of, e.g., biological interest where an intra-unit dynamics is added. If rather than actual unit-displacements, relative displacements, $\xi_n = x_{n+1} - x_n$, are considered, then Eqs. (1) become

$$\ddot{\xi}_n = U'(\xi_{n+1}) - 2U'(\xi_n) + U'(\xi_{n-1}). \tag{2}$$

The paradigmatic interaction potential introduced by Toda is

$$U(\xi_n) = -\frac{a}{b}\left[e^{-b(\xi_n - \sigma)} + b(\xi_n - \sigma) - 1\right], \tag{3}$$

where $\sigma$ is the mean equilibrium interparticle distance; $a > 0$ and $b > 0$ are parameters; $b$ accounts for the non-Hookean stiffness of the "springs" in the lattice; the last term $(-1)$ is added for computational convenience and need not to be included. Note that with $ab$ finite for $b \to 0$, the function (3) becomes the harmonic potential (linear Hookean "springs" for a standard crystal lattice) and $\omega_0^2 \equiv ab/m$ defines the angular frequency of vibrations in the harmonic limit. In the extreme opposite case $b \to \infty$, the potential (3) approaches the hard-rod/sphere limit (fluid-like system). Note also that under an external force or for finite temperatures the lattice constant equilibrium distance may not correspond to the minimum of the potential. Figure 1 shows the Toda potential adequately compared with Morse and Lennard-Jones potentials of current use in Physics and Chemistry. In what follows consideration will be given only to strong interparticle

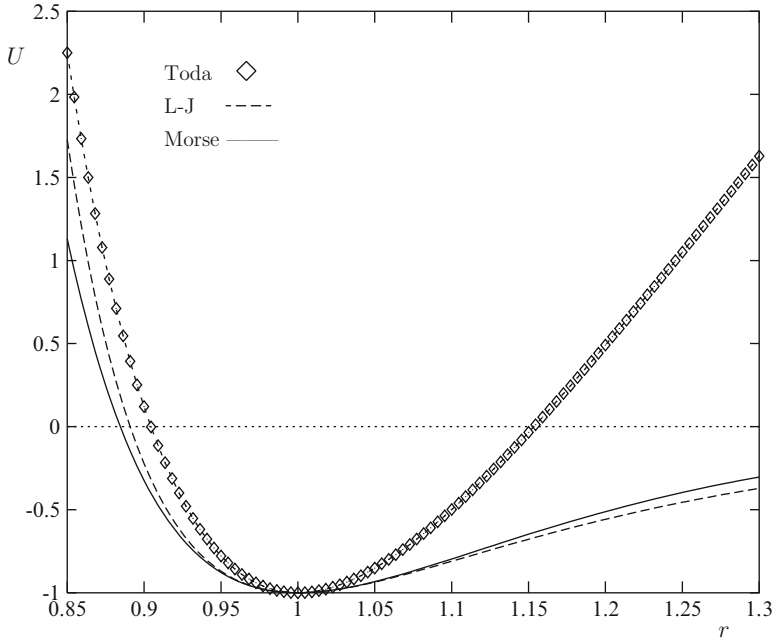


**Fig. 1** Rescaled representation with a common minimum (using $r$ rather them $x$) of the Toda potential $\left(U = U^T = \frac{a}{b}\left[e^{-b\sigma(r-1)} + b\sigma\,(r-1) - 1\right]\right)$, Morse potential $\left(U = U^M = \frac{a}{2b}\left[\left(e^{-b\sigma(r-1)} - 1\right)^2 - 1\right]\right)$ and Lennard-Jones potential $\left(U = U^{L-J} = U_0\left[\frac{1}{r^{12}} - \frac{1}{r^6} - 1\right]\right)$

compressions such that $\xi \leq \sigma/2$ (for simplicity $\sigma = 1$). Materials are usually stronger when compressed and weaker when stretched. In view of this, the fact that the attractive part of Toda's potential (3) is unphysical is of no concern to the study here.

For any finite value of $b$, in the infinite lattice, the equations of motion (2) possess a one-parameter family of soliton solutions

$$\xi_n = \sigma - 1\,(1/b)\,\ell n\left[1 + \sinh^2\kappa \mathrm{sech}^2\,(\kappa n \mp \sinh\kappa)\,\omega t\right]. \tag{4}$$

Inverting the logarithm it is just the sech$^2$ for $e^{-b(\xi_n - \sigma)}$. This exponential is related to the force (3) and characterizes the strength of the solitonic pulse. The parameter $\kappa$ controls the wave velocity and by the same token the wave amplitude (higher solitons travel faster),

$$v_{soliton}(\kappa) = \pm\omega_0\,(\sinh\kappa)\,/\kappa, \tag{5}$$

which in dimensionless units shows its supersonic character as the linear sound velocity is here given by $v_{sound} = \omega_0$ (positive and negative signs merely give

direction of wave propagation). When a periodic hence finite lattice is considered the exact solution of the equations of motion is a periodic "cnoidal" wave formed with Jacobian elliptic functions and complete elliptic integrals of the first and second kind (Toda 1989). It can be shown that in the *continuum* limit the solution of the discrete lattice can be approximated by the *cnoidal* solution of the Boussinesq-Korteweg de Vries equation (Boussinesq 1877; Korteweg and Vries 1895; Nekorkin and Velarde 2002) and in another limit by the solitary wave solution in the form of $\mathrm{sech}^2$. When the lattice has fixed constant length, as expansion is not permitted, experiences internal stress (pressure). If, however, the lattice length is free but no external force to it is applied (like compression or stretching at a free end), it can be shown that the lattice expands as it vibrates. The solitary wave is a *compression* pulse, and cnoidal waves cause expansion with, however, high compression at each periodic wave "peak" (or maximum). The exact wave dispersion relation of the Toda lattice is known explicitely.

Incidentally, the Toda lattice cannot sustain a thermal gradient although it permits a temperature difference, hence it is "transparent" to heat (solitons with exponential interaction like (3) run freely in the Toda lattice). This problem does not arise with Lennard-Jones interactions. In view of this, use is to be done of an *imperfect* Toda lattice and, recalling that interest here focused only on rather-strong lattice compressions, this can be achieved by substituting (3) with an *adapted* (non-integrable, hence imperfect) Toda-Morse lattice whose solutions and corresponding features should not differ significantly from the exact Toda solutions given above (Chetverikov et al. 2006; Dancz and Rice 1977; Rolfe et al. 1979). Thus rather than (3) we shall use:

$$U_M(\xi) = D\left[e^{-B(\xi-\sigma)} - 1\right]^2. \tag{6}$$

The specific heat at constant length/volume of the Toda lattice was obtained long ago (Toda 1989). The high-temperature limit $C_L = 0,5$ corresponds well with the fluid-like, hard-sphere phase. Then around $T = 1$, $C_L \approx 0,75$ it is the *soliton* range ($T$ unit: 2D; see below for further scalings). Well below $T = 1 = T_{transition}$, phonons (Fourier modes) control the thermodynamics (and dynamics) of the system. Similar phenomena can be observed in the dynamical structure factor (DSF) (typical for *inelastic* thermal neutron scattering experiments, $4\,\text{Å} \sim 5\,\text{meV} \sim 60\,\text{K}$ even up to $0.3\,\text{Å} \sim 0.1\,\text{eV} \sim 10^3\,\text{K}$). The latter is the double Fourier transform of the density-density correlation. When $T$ is well below $T = T_{transition}$ a single phonon peak appears that provides the linear sound velocity. As the transition temperature is approached from below the phonon spectrum gets multipeaked with many phonons or highly deformed phonons showing up (multiphonon range), until a much higher peak clearly emerges above a messy background. It corresponds to the soliton with supersonic velocity (5). Both the specific heat and DSF point to the significant role played by strong lattice compressions leading to solitons (Chetverikov et al. 2006).

## 2 Electron Capture and Electron Transfer

### 2.1 The Solectron Concept

If we now consider that lattice units are atoms with electrons and we add an *excess* electron we can consider two possibilities, one is electron transfer (ET) from a donor (D) to an acceptor (A) as schematized in Fig. 2 (Velarde et al. 2010a). The other possibility is electric transport or current in the presence of an external electric field. In both cases we have to follow the time evolution of the electron coupled to that of the lattice units, one affects the other. In the simplest form we can use the tight binding approximation (TBA) hence placing the electron at a lattice site and allowing electron hopping to nearby sites. In the TBA the time evolution of the electron follows the Schrödinger equation (for the lattice "space") augmented with the coupling with the anharmonic lattice, that reduces to

$$\mathrm{i}\hbar\dot{c}_n = E_n c_n - (V_{n,n-1}c_{n-1} + V_{n+1,n}c_{n+1})\,, \tag{7}$$

where the coupling of electron (normalized) probability density (amplitude, $|c_n|^2$) to lattice variables implicit in the $V_{n,m}$ appears. The choice

$$V_{n,\,n-1} = V_0 e^{-\alpha(\xi_n - \xi_{n-1})}, \tag{8}$$

is of current use dealing with, e.g., biomolecules. The parameter $\alpha$ is an inverse characteristic "length" scale.

To have a universal description suffices to make quantities dimensionless by introducing suitable scales/units: $\tau = V_0/\hbar\omega_M$, $\tilde{\alpha} = \alpha/B$, and $\tilde{V} = V_0/2D$ thus using the depth of the Morse potential as unit/scale; $\omega_M = \left(DB^2/M\right)^{1/2}$, $M$ denotes lattice units mass (typical parameter values for some biomolecules (Gray and Winkler 2003, 2005) are: $B = 4.45\,\text{Å}^{-1}$, $\alpha = 1.75B$, $D = V_0 = 0.1\,\text{eV}$, $\omega_M = 3.10^{12}\,\text{s}^{-1}$, $V_0/\hbar = 0.6\cdot 10^{14}\,\text{s}^{-1}$, $\tau = 10$). Then we can rewrite (7) as

$$\mathrm{i}\dot{c}_n = -\tau\left[e^{-\alpha(\xi_n - \xi_{n-1})}c_{n-1} + e^{-\alpha(\xi_{n+1} - \xi_n)}c_{n+1}\right]. \tag{9}$$

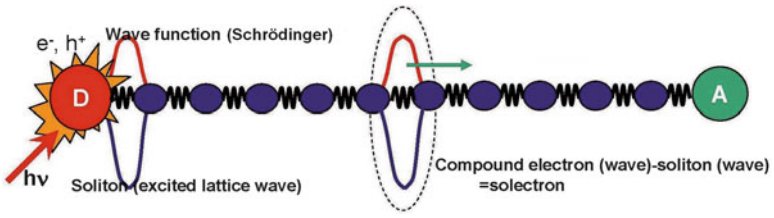


**Fig. 2** ET along a biomolecule modeled by a lattice. The excess electron (wave function $\Psi$) is emitted from site **D** (donor) by appropriate energy supply and travels along the bridge or "backbone" lattice made of *anharmonic* elements down to the site **A** (acceptor)

The parameter $\tau$ shows explicitely the time scale of electron motions while the time $t$ corresponds to the slower time scale of the lattice vibrations. The latter obey the Eq. (2) augmented with the coupling to electron *hopping* motions or better said, electron probability coefficients,

$$\ddot{\xi}_n = \left[1 - e^{(\xi_{n+1}-\xi_n)}\right] e^{-(\xi_{n+1}-\xi_n)} - \left[1 - e^{-(\xi_n-\xi_{n-1})}\right] e^{-(\xi_n-\xi_{n-1})} - \\ -\alpha V \left[\left(c^*_{n+1}c_n + c_{n+1}c^*_n\right) e^{-\alpha(\xi_{n+1}-\xi_n)} + \left(c^*_n c_{n-1} + c_n c^*_{n-1}\right) e^{-\alpha(\xi_n-\xi_{n-1})}\right]. \tag{10}$$

Clearly, the interplay between electron and lattice vibrations has now a genuinely new element, the soliton-mediated effect. This permits to consider the compound electron-soliton "quasiparticle", due to its "universal" carrier character, as a new physical entity which is the "solectron" one way of providing electron "surfing" on a subsonic/supersonic sound (longitudinal lattice soliton) wave (Cantu Ros et al. 2011; Velarde 2010).

## 2.2 Soliton Electron Trapping

Consider an electron placed at site "$n$" in a lattice. Then let alone the electron, its evolution is dictated by Eq. (9) with $\alpha = 0$. Figure 3 shows how from an initially peaked probability density as time proceeds the probability spreads down to a uniform distribution over all lattice sites and hence ends up by being *completely delocalized*.

Other evolution possibilities have been explored (Hennig et al. 2006, 2007). Taking now Eq. (2) and launching as an initial condition a soliton at a certain lattice site and then switching-on the electron-lattice interaction hence switching-on Eq. (10), for an initial condition of the electron completely *delocalized*, and then operating Eq. (9) in full, the striking result found is illustrated in Fig. 4. Subsequently, after trapping the electron, the compound or bound state soliton-electron, i.e., the *solectron* proceeds moving unaltered along the lattice.

When two solitons which are allowed to collide in their evolution along the lattice are launched and the electron starts being trapped and carried by one of the solitons, e.g. by the one moving left-to-right, then as the collision proceeds and "finishes", the electron may leave the first soliton and reappear trapped and carried by the second soliton. Accordingly, the electron may change both partner and direction of motion after the collision. Another striking result also observed numerically is the electron probability density splitting thus illustrating how quantum mechanically the electron (in probability sense) can move simultaneously! in both directions (Velarde et al. 2008a).

If an external electric field is acting there is current, it suffices to add to Eq. (9) the term $(-n\mathbf{E}c_n)$ and then to compute

$$j = \mathrm{i} \sum \left(c^*_{n+1}c_n - c^*_n c_{n-1}\right), \tag{11}$$

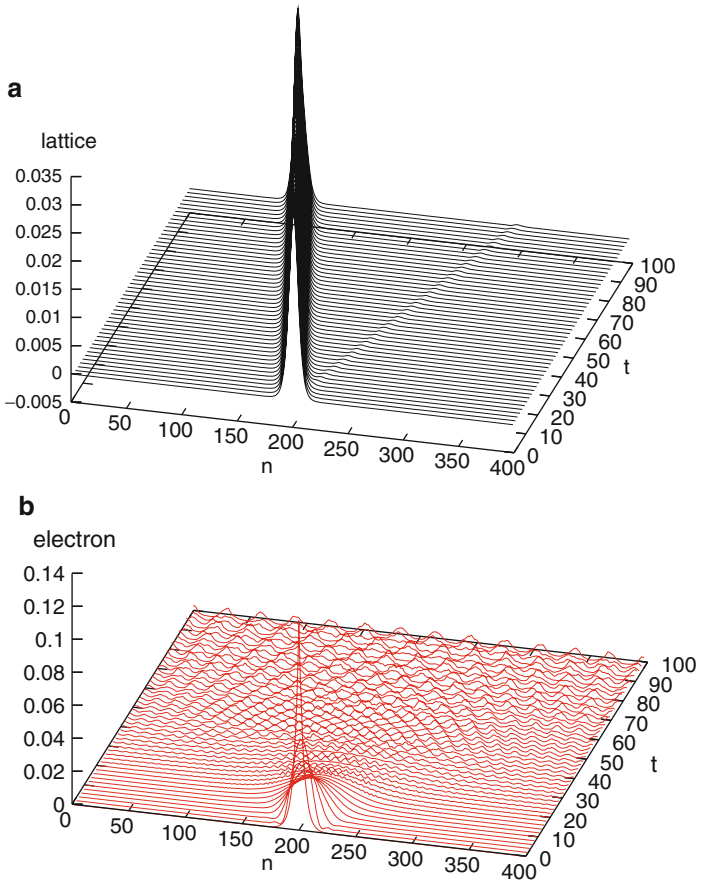


**Fig. 3** Soliton and electron taken separately (no interaction). (**a**) lattice soliton time evolution starting at site $n = 200$. (**b**) Electron probability density time evolution. From initial "localization" at site $n = 200$ the electron ends up *completely delocalized*, i.e., the proability density is spread "uniformly" everywhere along the lattice

which then depends on the external field strength. This is apparently so but not always in reality. Indeed, for high enough field strength it can be seen that the latter forces the electron to follow Ohm's law. But as the field strength becomes low enough it is rather the soliton which commands the electric current which becomes field-independent thus remaining constant as the field strength tends to zero. This striking result is not unexpected if we recall what the "soliton" wave does to a surfer.

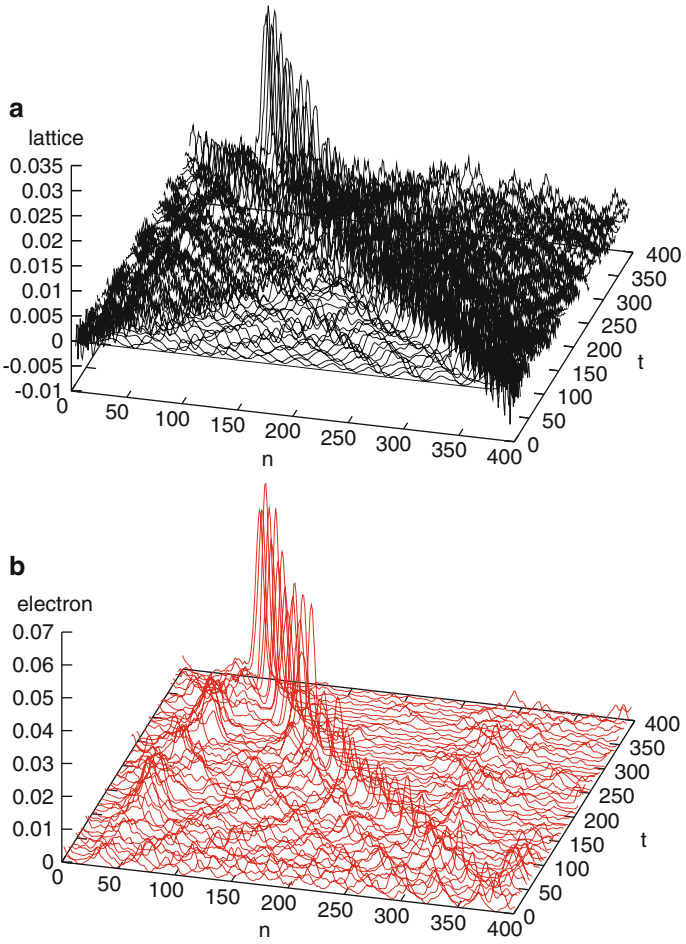


**Fig. 4** Interaction of a *soliton* with a *completely delocalized* electron. *Right figure*: the electron after following evolution dictated by Schrödinger equation ends up *completely delocalized* with probability density spread like "dust" over the entire lattice. Then at such time instant the soliton is launched taking as initial condition for the electron the final state of the right picture in Fig. 3. *Left figure*: the soliton after gathering the electron dusty probability density eventually reconstructs the electron probability density in a kind of "vacuum cleaner" process

## 3 Heated Crystal Lattices

So far no mention was done of temperature other than when referring to the specific heat (Fig. 5). Strictly speaking the results described above hold at zero-K. Let us now consider that the system is heated-up from zero-K to the soliton range ($T \approx 0.1-1$) defined in Fig. 5. The heating can be done by a suitable thermal bath satisfying Einstein's relation between noise strength and equivalent temperature in K. As we

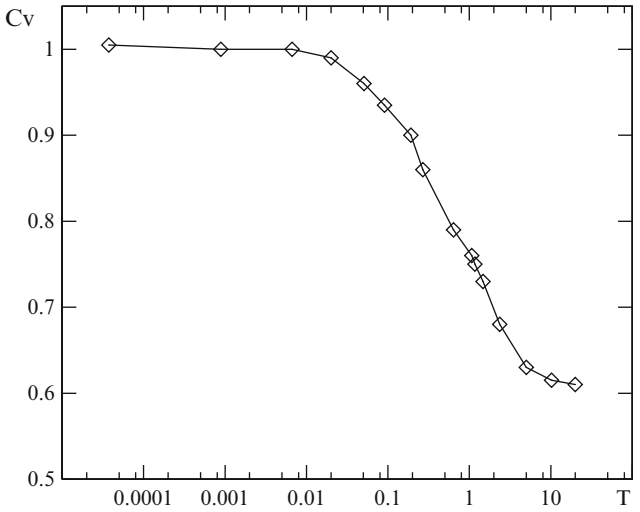


**Fig. 5** Specific heat at constant length/volume in $k_B$ units. $T_{transition} = 1$, for which here $C_L \equiv C_v = 0.75$. $C_v = 1$ is the Dulong-Petit (Einstein) value (solid phase; harmonic interaction) and $C_v = 0,5$ corresponds to the fluid-like phase (hard-rod interaction). Missing in the figure is the low temperature values arising from genuinely quantum mechanics ($T^d$ Debye law with $d$ denoting space dimension)

shall continue restricting consideration to 1d lattices let us recall the Hamiltonian, $H_a$, using $x_n$ as lattice coordinates. Then we have

$$H_a = \frac{m}{2}\sum_{n=1}^{N} v_n^2 + \frac{1}{2}\sum_{n,i=1}^{N} U\,(x_n, x_i), \tag{12}$$

where $v_n$ denote velocities, and $U$ corresponds to the Morse potential (6) (Fig. 1). Then in the presence of random forces (hence nonzero temperature) and also external forces the evolution of lattice particles is given by the Langevin equations

$$\frac{d}{dt}v_n + \frac{1}{m}\frac{\partial H_a}{\partial x_n} = -\gamma_0 v_n + \sqrt{2D_v}\,\xi_n(t). \tag{13}$$

The stochastic forces $\sqrt{2D_v}\,\xi_n(t)$ define a time delta correlated Gaussian white noise. The parameter $\gamma_0$ describes the standard friction frequency acting from the bath. The Einstein relation is $D_v = k_B T\gamma_0/m$, where $T$ denotes absolute temperature and $k_B$ is Boltzmann's constant.

In order to visualize the solitons we can focus attention to the "atomic" density. We assume that each lattice unit is surrounded by a Gaussian electron density providing a screened ion core of width $s = 0.35\sigma$. Then the total atomic electron density, defining a lattice unit, is given by

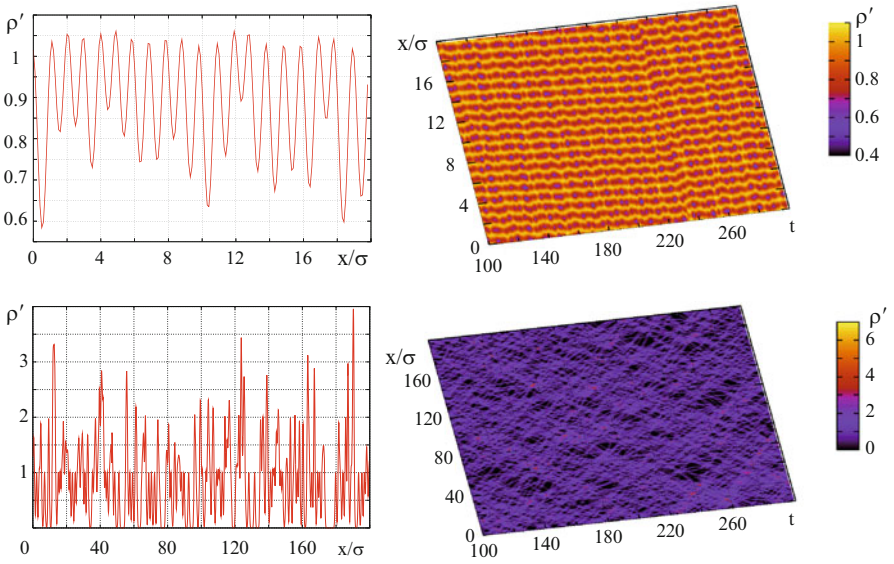


**Fig. 6** Visualisation of soliton-like running excitations. Density $\rho' = \rho\sqrt{2\pi}s$ refers to electrons in lattice atoms (color coding in arbitrary units). $N = 200, B\sigma = 1, s = 0.35\sigma$. For two temperatures (given in units of $2D$) we have: *Upper set of figures*: (i) $T = 0.005$: Only harmonic lattice vibrations show up with no evidence of soliton-like excitations; and *bottom set of figures*: (ii) $T = 1$: Besides many excitations also a few strong solitons appear running with velocity around $1.3v_{sound}$. In both cases a snapshot of the distribution for a certain time instant and the actual time evolution of the distribution are displayed

$$\rho(x) = \sum_n \frac{1}{\sqrt{2\pi}s} \exp\left[-\frac{(x - x_n(t))^2}{2s^2}\right]. \tag{14}$$

Hence we assume that the atom is like a spherical object with continuous electron density concentrated around each lattice site. In regions where the atoms overlap, the electron density is enhanced. This permits easy visualization of soliton-like excitations based on the colors in a density plot. This is of course a rough approximation. Figure 6 shows the result of simulations for the temperatures $T = 0.005$ and $T = 1$. The diagonal stripes correspond to regions of enhanced density which are running along the lattice. This is a sign of solitonic excitations. Checking the slope we see excitations which over 10 time units move with *supersonic* velocity. We have solitonic excitations living about 10–50 time units corresponding to $1-3$ ps. Besides they survive even at $T = 1$ which is well above the physiological temperature (about 300 K which is above $T \approx 0.1$ with $D \simeq 0.1$ eV). Due to lack of space we shall not discuss here the solectron survival as we heat the lattice. The formation of solectron occurs as indicated above and does survive as a compound up to such temperatures. For details we refer the reader to the analyses presented in Chetverikov et al. (2009, 2010, 2012), Ebeling et al. (2009), and Velarde et al. (2008b).

## 4 Two-Dimensional Soliton-Like Excitations

Let us now extend the study to the case of a two-dimensional (2d) lattice still with Morse interactions. The lattice Hamiltonian (12) becomes now

$$H_a = \frac{m}{2}\sum_n v_n^2 + \frac{1}{2}\sum_{i,j} V(r_i,\, r_j). \tag{15}$$

The subscripts locate atoms at lattice sites $n$ with coordinates $(i, j)$ and the summations run from 1 to $N$. As before the characteristic distance determining the repulsion between the particles in the lattice is $\sigma$. We limit ourselves to nearest-neighbors only using the relative distance $r = |r_n - r_k|$. The Morse potential (Fig. 1) if for convenience, expressed as

$$U_M = D\left\{\exp[2B(r-\sigma)] - 2\exp[-B(r-\sigma)]\right\}. \tag{16}$$

In order to avoid unphysical cumulative interaction effects, a suitable cut-off rules out a stronger interaction than due arising from the influence of particles outside the first neighborhood of each particle. In fact, rather than a cut-off we consider the interaction with a smooth decay to zero as distance increases. Hence rather than (16) for the 2d lattice we take

$$\begin{aligned} U_M(r) = 2D\left\{\exp\left[-2b(r-\sigma)\right] - 2\exp\left[-b(r-\sigma)\right]\right\}\cdot \\ \cdot\left\{1+\exp[(r-d)/2\nu]\right\}^{-1}. \end{aligned} \tag{17}$$

As a rule the cut-off "interaction radius" is supposed to be equal to $1.5\sigma$, together with parameter values $d = 1.35\sigma$ and $\nu = 0.025$. Beyond the cut-off radius the potential is set to zero. To study, at varying temperature, the nonlinear excitations of the lattice and the possible electron transport in a lattice it is sufficient to know the lattice (point) particles coordinates at each time and the potential interaction of lattice deformations with electrons. The former are obtained by solving the equations of motion of each particle (15) under the influence of all possible forces. The latter include forces between particles which are supposed to be of the Morse kind and the friction and random forces accounting for a Langevin model bath in the heated lattice. We use complex coordinates $Z = x + iy$, where $x$ and $y$ are Cartesian coordinates for each $r$. Then the Langevin equations (13) for the lattice units, $n$, become now

$$\frac{d^2 Z_n}{dt^2} = \sum_k F_{nk}(Z_{nk}) z_{nk} + \left[-\gamma\frac{Z_n}{dt} + \sqrt{2D_v}\left(\xi_{nx} + i\xi_{ny}\right)\right], \tag{18}$$

where $\gamma$, $D_v$ and $\xi_{nx,y}$ have earlier defined roles. $Z_{nk} = Z_n - Z_k$, then $z_{nk} = (Z_n - Z_k)/|Z_n - Z_k|$ is a unit vector defining the direction of the interaction force $F_{nk}$.

To have dimensionless variables we consider the spatial coordinates normalized to the length $\sigma$. The energy is scaled with $2D$. The interaction force $F_{nk}$ is given by

$$F_{nk} = F_{nk}(|Z_{nk}|) = -\frac{dV(r)}{dr}|_{r=|Z_{nk}|}. \tag{19}$$

In view of the above only those lattice units with coordinates $Z_k$, satisfying the condition $|Z_n - Z_k| < 1.5$, are taken into account in the sum in Eq. (18). In computer simulations the interaction of particles is considered to take place inside a rectangular cell $L_x \cdot L_y$ with periodic boundary conditions and $L_{x,y}$, depending on the symmetry of an initial distribution of units and their number $N$. For illustration we consider a distribution corresponding to the minimum of potential energy for an equilibrium state of a *triangular* lattice $10\sigma \cdot 10\sqrt{3/2}\sigma$ for $N = 100$ or $20\sigma \cdot 20\sqrt{3/2}\sigma$ for $N = 400$.

As in the preceding Section, we will assume that the atomic electrons may be represented by a Gaussian distribution centered on each lattice site:

$$\rho(Z,t) = \sum_{|Z-Z_i(t)|<1.5} \exp\left[-\frac{|Z - Z_i(t)|^2}{2\lambda^2}\right]. \tag{20}$$

In Fig. 7 we show the evolution of one localized soliton-like excitation in a triangular Morse lattice. The initial form of the excitation is a small piece of a plane soliton-like wave with a front oriented along one of symmetry axes of a triangular lattice and a velocity directed along an other axis (x-axis here). The density distribution (left column), and the cumulated during the time mentioned at each row amplitude-filtered density-distribution (right column) are presented for three time instants. We observe the transformation of the initial piece of a plane wave to a soliton-like horseshoe-shaped supersonic excitation. As the excitation travels a distance of about 16 units in the time internal $t = 8$, its supersonic velocity is $16/8 = 2$ in units of the sound velocity in 1D lattice. Note that $v_{sound} = 1$ for 1d-lattices. In a 2d-triangular lattice the sound velocity is $\sqrt{2} \simeq 1.4$ times higher than the sound velocity in a 1d-lattice.

In a subsequent set of simulations we studied two solitons excited initially, the left one propagating to the right, the right one – to the left. The parameter values are the same as in the one-soliton case above. We have observed first a transformation of the initial pieces of a plane wave to a 2d horseshoe-shaped soliton-like wave fronts and then both moving head-on against each other. Looking at Fig. 8 we observe that the two localized and supersonic excitations pass through each other without changing their form. This is a signature of solitons. They are not solitons in the rigorous mathematical sense because we do not prove that they are exact stationary waves (indeed our 2d excitations are "long lasting" transitory waves) but clearly their behavior is like that of surface solitons observed in fluids (Chetverikov et al. 2011b,c; Nepomnyashchy et al. 2002).

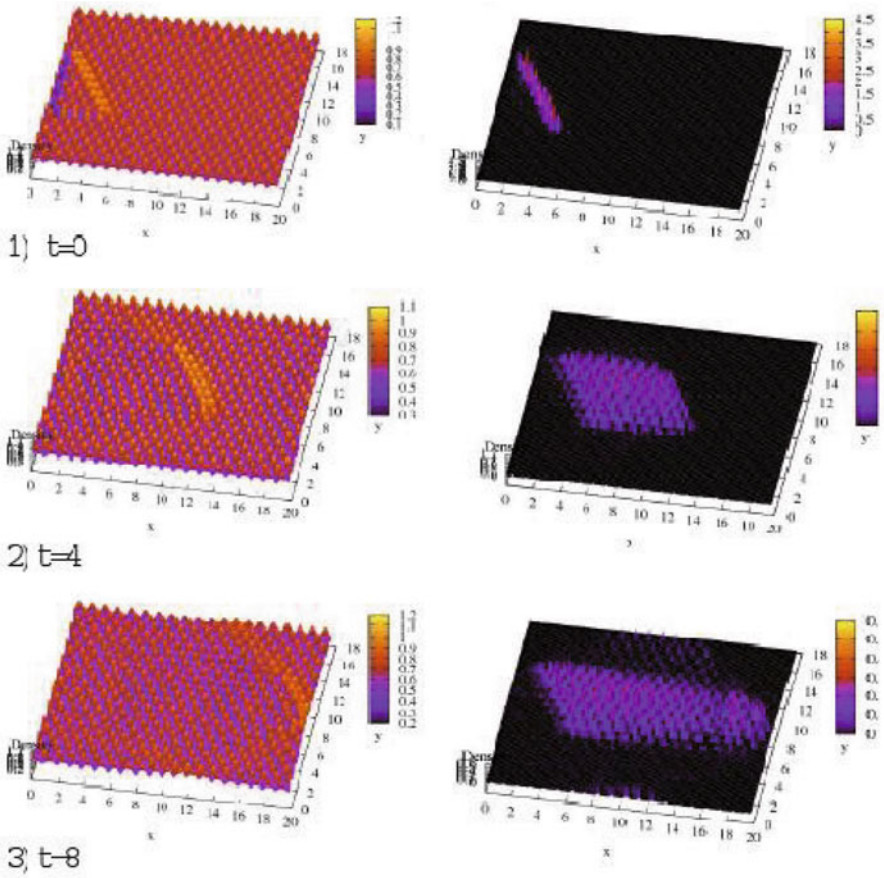


**Fig. 7** Propagation of soliton-like excitation in a triangular lattice. *Left column*: density of the atom cores. *Right column*: a cumulated representation at final time. In order to study the evolution of perturbations we changed the initial positions of the atoms at $t = 0$ in a small region. Parameter values: $N = 400$, $b\sigma = 4$, $\lambda = 0.3$, $T = 0.01$

We have also studied the role of heating and hence observing excitations at finite temperatures. As we have no space to discuss this problem here we refer the reader to Chetverikov et al. (2011a).

## 5 Conclusion

We have succintly discussed features of solitons in 1d and 2d anharmonic crystal lattices and, in particular, some consequences of heating the system. We have also discussed features of coupling lattice solitons to added *excess* electrons leading to

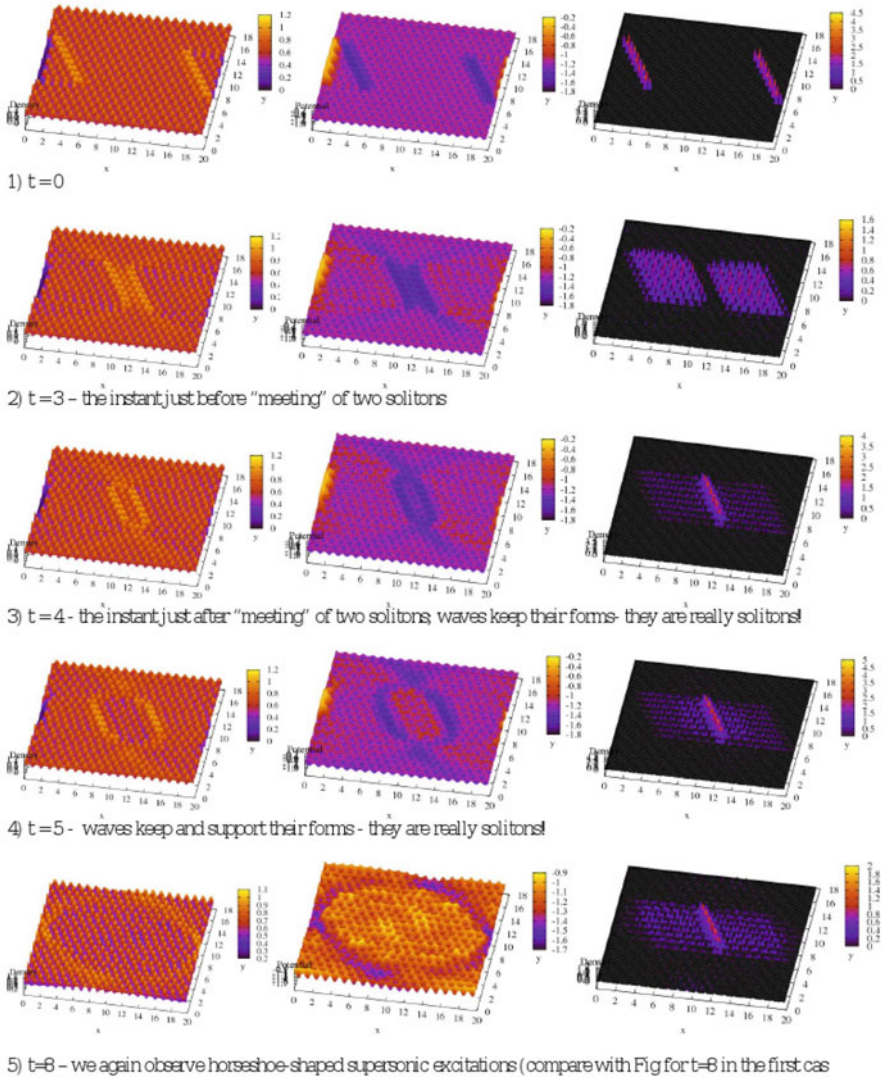


**Fig. 8** Triangular lattice: Head-on collision of two oppositely moving solitons in the interval $t = 0 - 8$, both with the same parameters values: $N = 400$, $b\sigma = 4$, $\lambda = 0.3$, $T = 0.01$

the formation of bound states or compounds electron-soliton, denoted solectrons. Recently, we have also studied, albeit only in the 1d case, the formation of electron pairs (with opposite spins satisfying Pauli's exclusion principle and experiencing Coulomb repulsion using Hubbard's local approximation) (Hennig et al. 2008; Velarde and Neissner 2008; Velarde et al. 2010b, 2012). Finally, three recent experiments have provided collateral verification of the major predictions of the

theory here presented. One (Slinker et al. 2011) provides evidence of *ballistic* transport in synthetic DNA and the other two (Hermelin et al. 2011; McNeil et al. 2011) (see also Chetverikov et al. (2012) and Nayanov (1986)) provide evidence of electron "surfing" on sound waves in piezoelectric *GaAs*. Further details about comparison between theory and experiments would be provided elsewhere.

**Acknowledgements** The authors are grateful to A.S. Alexandrov, E. Brändäs, L. Brizhik, L. Cruzeiro, F. de Moura, J. Feder, D. Hennig, R. Lima, R. Miranda, R. McNeil, G. Röpke and G. Vinogradov for enlightening discussions. This research has been sponsored by the Spanish Ministerio de Ciencia e Innovacion, under Grants EXPLORA-FIS2009-06585-E and MAT2011-26221.

## References

Boussinesq, J.V.: Mem. presentes par divers savants a l'Acad. Sci. Inst. France (Paris) **23**, 1 (1877); ibidem **24**, 1 (1878), Eq. (283 bis)
Cantu Ros, O.G., Cruzeiro, L., Velarde, M.G., Ebeling, W.: Eur. Phys. J. B **80**, 545 (2011)
Chetverikov, A.P., Ebeling, W., Velarde, M.G.: Int. J. Bifurc. Chaos **16**, 1613 (2006)
Chetverikov, A.P., Ebeling, W., Velarde, M.G.: Eur. Phys. J. B **70**, 217 (2009)
Chetverikov, A.P., Ebeling, W., Velarde, M.G.: Int. J. Quantum Chem. **110**, 46 (2010)
Chetverikov, A.P., Ebeling, W., Velarde, M.G.: Eur. Phys. J. B **80**, 137 (2011a)
Chetverikov, A.P., Ebeling, W., Velarde, M.G.: Phys. D **240**, 1954 (2011b)
Chetverikov, A.P., Ebeling, W., Velarde, M.G.: Wave Motion **48**, 753 (2011c)
Chetverikov, A.P., Ebeling, W., Velarde, M.G.: Eur. Phys. J. B **85**, 291 (2012)
Dancz, J., Rice, S.A.: J. Chem. Phys. **67**, 1418 (1977)
del Rio, E., Velarde, M.G., Ebeling, W.: Phys. A **377**, 435 (2007)
Ebeling, W., Velarde, M.G., Chetverikov, A.P.: Condens. Matter Phys. **12**, 633 (2009)
Fermi, E., Pasta, J.R., Ulam, S.: Los Alamos Nat. Lab. Report LA-1940 (1955); In: Collected Papers of Enrico Fermi, pp. 978–988. University of Chicago Press, Chicago (1965)
Gray, H.B., Winkler, J.R.: Q. Rev. Biophys. **36**, 341 (2003)
Gray, H.B., Winkler, J.R.: Proc. Natl. Acad. Sci. **102**, 3534 (2005)
Hennig, D., Neissner, C., Velarde, M.G., Ebeling, W.: Phys. Rev. B **73**, 024306 (2006)
Hennig, D., Chetverikov, A.P., Velarde, M.G., Ebeling, W.: Phys. Rev. E **76**, 046602 (2007)
Hennig, D., Velarde, M.G., Ebeling, W., Chetverikov, A.P.: Phys. Rev. E **78**, 066606 (2008)
Hermelin, S., Takada, S., Yamamoto, M.: Nature **477**, 435 (2011)
Korteweg, D.J., de Vries, G.: Philos. Mag. **39**, 442 (1895)
McNeil, R.P.G., Kataoka, M., Ford, C.J.B., Barnes, C.H.W., Anderson, D., Jones, G.A.C., Farrer, I., Ritchie, D.A.: Nature **477**, 439 (2011)
Nayanov, V.I.: JETP Lett. **44**, 314 (1986)
Nekorkin, V.I., Velarde, M.G.: Synergetic Phenomena in Active Lattices. Patterns, Waves, Solitons, Chaos. Springer, Berlin (2002). Chap. 1
Nepomnyashchy, A.A., Velarde, M.G., Colinet, P.: Interfacial Phenomena and Convection. Chapman & Hall/CRC, London (2002). Chap. 5.
Payton, D.N. III, Rich, M., Visscher, W.M.: Phys. Rev. **160**, 706 (1967). See also Proceedings International Conference on Localized Excitations in Solids, pp. 657–664. Plenum, New York (1968)
Rolfe, T.J., Rice, S.A., Dancz, J.: J. Chem. Phys. **70**, 26 (1979)
Slinker, J.D., Muren, M.B., Renfrew, S.E., Barton, J.K.: Nat. Chem. **3**, 228 (2011)
Toda, M.: Theory of Nonlinear Lattices, 2nd edn. Springer, Berlin (1989)

Velarde, M.G., J. Comput. Appl. Math. **233**, 1432 (2010)
Velarde, M.G., Neissner, C.: Int. J. Bifurc. Chaos **18**, 885 (2008)
Velarde, M.G., Ebeling, W., Chetverikov, A.P., Hennig, D.: Int. J. Bifurc. Chaos **18**, 521 (2008a)
Velarde, M.G., Ebeling, W., Chetverikov, A.P.: Int. J. Bifurc. Chaos **18**, 3815 (2008b)
Velarde, M.G., Chetverikov, A.P., Ebeling, W., Hennig, D., Kozak, J.J.: Int. J. Bifurc. Chaos **20**, 185 (2010a)
Velarde, M.G., Ebeling, W., Chetverikov, A.P.: Int. J. Bifurc. Chaos **21**, 1595 (2010b)
Velarde, M.G., Brizhik, L., Chetverikov, A.P., Cruzeiro, L., Ebeling, W., Röpke, G.: Int. J. Quantum Chem. **112**, 551 (2012); ibidem 112, 2591 (2012)
Zabusky, N.J.: Chaos **15**, 015102 (2005)
Zabusky, N.J., Kruskal, M.D.: Phys. Rev. Lett. **15**, 57 (1965)